A glucose-dependent spatial patterning of exocytosis in human β-cells is disrupted in type 2 diabetes

Jianyang Fu[1], John Maringa Githaka[2], Xiaoqing Dai[1], Gregory Plummer[1], Kunimasa Suzuki[1], Aliya F. Spigelman[1], Austin Bautista[1], Ryekjang Kim[1], Dafna Greitzer-Antes[3], Jocelyn E Manning Fox[1], Herbert Y. Gaisano[3], Patrick E MacDonald[1]

[1]Alberta Diabetes Institute and the Department of Pharmacology, University of Alberta, Edmonton, AB, T6G 2E1, Canada

[2]Department of Biochemistry, University of Alberta, Edmonton, AB, T6G 2E1, Canada

[3]Departments of Medicine and Physiology, University of Toronto, Toronto, ON, M5S 1A8, Canada

Correspondence to:

Dr. Patrick MacDonald
Alberta Diabetes Institute
LKS Centre, Rm. 6-126
University of Alberta
Edmonton, AB
Canada, T6G 2E1
pmacdonald@ualberta.ca
www.bcell.org

KEYWORDS: diabetes, islets of Langerhans, insulin, exocytosis, ion channels, SUMOylation

SUMMARY

Impaired insulin secretion in type 2 diabetes (T2D) is linked to reduced insulin granule docking, disorganization of the exocytotic site, and an impaired glucose-dependent facilitation of insulin exocytosis. We show in β-cells from 80 human donors that the glucose-dependent amplification of exocytosis is disrupted in T2D. Spatial analyses of granule fusion events, visualized by total internal reflection fluorescence (TIRF) microscopy, demonstrate that these are non-random across the surface of β-cells from donors with no diabetes (ND). The compartmentalization of events occurs within regions defined by concurrent or recent membrane-resident secretory granules. This organization, and the number of membrane-associated granules, is glucose-dependent and notably impaired in T2D β-cells. Mechanistically, multi-channel Kv2.1 clusters contribute to maintaining the density of membrane-resident granules and the number of fusion 'hot spots', while SUMOylation sites at the channel N- (K145) and C-terminus (K470) determine the relative proportion of fusion events occurring within these regions. Thus, a glucose-dependent compartmentalization of fusion, regulated in part by a structural role for Kv2.1, is disrupted in β-cells from donors with type 2 diabetes.

Abstract: 172 words; Main text: 7485 words (text, references, legends); Figures: 7; References: 56

HIGHLIGHTS

- Exocytosis of secretory granules is non-random across the surface of human β-cells, and this organization is disrupted in type 2 diabetes.
- Increasing glucose facilitates the spatial compartmentalization of fusion, independent of an overall increase in event frequency.
- Compartmentalized 'hot spots' occur at sites marked by membrane-associated granules, the density of which is regulated in part by a clustered K^+ channel (Kv2.1).
- SUMOylation status of the channel controls the proportion of events that occur within these local regions.

INTRODUCTION

Insulin, secreted from pancreatic islet β-cells, is a critical regulator of blood glucose and energy homeostasis in humans (1). Impaired insulin secretion is a hallmark of type 2 diabetes (T2D) which results from a complex interplay between reduced insulin sensitivity and impaired insulin secretion (2). A tipping point occurs when secretion from genetically predisposed β-cells fails to compensate for insulin resistance (3, 4). While impaired insulin responses in T2D may result from a long-term reduction in β-cell mass (5), reduced secretory function likely predominates at earlier stages (6, 7). Importantly, exocytotic protein expression is reduced in islets from human donors with T2D (8, 9) and exocytotic responses are impaired at the single-cell level (10, 11). Most recently this has been attributed to an impaired glucose-dependent granule docking and reduced expression of docking and related active zone proteins (12)

The spatiotemporal organization of fusion events within pancreatic β-cells, particularly those of human donors, is not well studied. While neurotransmitter release is compartmentalized at the active zone of the presynaptic nerve terminus, β-cells lack ultra-structurally identifiable active zones. These cells are however polarized and glucose-stimulation triggers release events that are progressively localized to preferential release sites (13) which appear directed towards the islet vasculature (13-16). Since active zones in neuronal synapses are composed of conserved protein complexes containing ion channels and SNARE proteins similar to β-cells, such as Munc13 and RIM2 (regulating synaptic membrane exocytosis protein 2) (17), and voltage-dependent Ca^{2+} channels (18), areas analogous to active zones may contribute to regulated exocytosis in pancreatic β-cells. In insulinoma cells and rodent β-cells, individual vesicle fusion events are apparently not random and exocytosis may occur at sites of recently fused vesicles (19-23). Indeed, syntaxin1A and SNAP-25 cluster at sites of secretory granule docking and exocytosis in β-cells (24, 25) and reduced SNAP-25 and syntaxin1A clusters correlates with impaired fusion (26). Also, fusion sites are localized to sites of Ca^{2+} entry in β-cells, and this interaction is disrupted in β-cells from models of T2D (27, 28) and β-cells of human donors with T2D (18). The extent to which fusion events can repetitively occur at defined 'hot spots' on the β-cell membrane, and the potential dysregulation of this in human T2D, remains unclear.

Among the ion channels that control β-cell function, the voltage-dependent L-type Ca^{2+} channels increase intracellular Ca^{2+} and trigger exocytosis (29). Repolarization of pancreatic β-cell action potentials is mediated by voltage-dependent K^+ (Kv) channels such as Kv2.1 (30). Interestingly, Kv2.1 also forms multi-channel clusters at the plasma membrane (31) that directly facilitate efficient insulin exocytosis (20, 32, 33), and may also may recruit SNARE complex proteins such as syntaxin1A, SNAP-25 and Munc18-1 (34). The channel regulates insulin exocytosis independent of β-cell electrical activity by binding syntaxin1A at its C-terminus (33, 35), a region that is modified by post-translational SUMOylation (36). Indeed, the glucose-regulated deSUMOylation of targets at the plasma membrane appears particularly important for the regulation of insulin secretion and control of glucose homeostasis (37, 38) and when stimulated can rescue exocytotic responses in human T2D β-cells (11).

Here we examined exocytotic responses from β-cells of 80 human donors with and without T2D. We demonstrate an impaired insulin secretion that can occur independent of a reduced islet insulin content in this cohort and confirm a cell-autonomous impairment in exocytotic function. By total internal reflection fluorescence (TIRF) microscopy and spatial analyses, we demonstrate a non-random distribution of fusion events across the cell membrane and show that this patterning is regulated by glucose and is disrupted in β-cells of donors with T2D. Knockdown of Kv2.1 reduces the spatial organization of these events, and we show that channel clustering controls the density of fusion 'hot spots' while the SUMOylation status of the channel at C- and N-terminal sites regulates the overall proportion of fusion events that occur at these sites. Finally, up-regulation of Kv2.1 in T2D β-cells can convert a random distribution of fusion events into a compartmentalized pattern similar to that seen in β-cells of donors without diabetes.

RESULTS

Impaired spatial patterning of fusion in β-cells from donors with T2D

Glucose-stimulated insulin secretion is impaired from islets of donors with type 2 diabetes (T2D) (6, 39). In a cohort of 80 human islet preparations (**Suppl. Tables 1-2**) we confirm that glucose-stimulated insulin secretion is impaired in T2D and show that this can occur without a reduction in insulin content (**Fig 1A-B**). Although we (40) and others (39) have reported reduced

islet insulin content from donors with long-standing T2D, the disease duration in these donors is relatively short (average 6.7 years, including some 'undiagnosed diabetes'). Donors with longer duration diabetes, or with higher HbA1c, tended to have lower islet insulin content (not shown). In these donors we find that while increasing glucose facilitates exocytosis in β-cells from donors with no diabetes (ND), seen as a rightward shift in the distribution of exocytotic responsiveness of these cells (**Fig 1C**), this is impaired in T2D (**Fig 1D**) consistent with a cell autonomous impairment in β-cell exocytosis regulation by glucose (11).

Impaired exocytosis in models of T2D is associated with an uncoupling of exocytosis from sites of Ca^{2+} entry (27, 28) and human T2D β-cells have a defect in glucose-dependent granule docking (12). We performed live-cell total internal reflection fluorescence (TIRF) microscopy to assess the spatial relationship of fusion events in cells from a subset of ND and T2D donors. To identify and perform spatiotemporal analysis of vesicle fusion, a MATLAB-based software (19) was applied to live-cell recordings obtained with 5 mM glucose in the bath solution for 2 minutes, following preincubation at 1 mM glucose for 30 minutes. Fusion events from ND β-cells had a higher degree of spatial organization than those observed in T2D β-cells, with numerous events appearing to occur repeatedly at 'hot spots' (**Fig 1E-J; Suppl Movie 1- 2**) within a defined area of 4x4 pixels determined by average vesicle diameter (see Methods). Each apparent hot spot was confirmed by generating event heat maps and comparing relative fluorescence to the first frame (**Fig 1F,I**). The spatial organization of events was also confirmed by calculating Ripley's K-function values, which demonstrate a non-random distribution of these events (**Fig 1G, J**). In ND β-cells 41.6% of events occur within spatially localized regions, while only 18.3% do so in T2D β-cells.

We confirmed impaired exocytosis by patch-clamp electrophysiology at 5 mM glucose (**Fig 1K**). Live-cell imaging of cells from the same donors under this condition for 2 mins (following a 1 mM glucose pre-incubation) reveals that accumulated fusion events are decreased 56.1% in the T2D β-cells (**Fig 1L**). Calculation of a Uniform Index (see Methods) demonstrates that fusion events in the ND β-cells showed significant compartmentalization ('observation') compared with Monte Carlo simulation of each cell assuming random distribution of events ('simulation'), or events in the T2D β-cells which were seen to be no more organized than random simulation (**Fig 1M**). While the above analyses account for differences in event frequency, we wished to confirm

that the differential organization of events occurs independently of an overall decreased exocytosis since event frequency correlates with the proportion occurring at 'hot spots' (**Fig 1N**).

Analysis of a sub-set of cells with equivalent exocytosis (dashed box and *inset*, **Fig 1N**) demonstrates that the proportion of events occurring at 'hot spots' (**Fig 1O**) and the density of these (**Fig 1P**) are decreased in T2D. Thus, impaired insulin secretion from islets of donors with T2D is associated with reduced exocytotic responses measured both by patch-clamp and live-cell imaging, and with an independent reduction in the compartmentalization of fusion events determined by generation of exocytotic heat maps, Ripley's K-function, Voronoi polygon-derived Uniform Index, and cell sub-set analyses.

Glucose-dependent spatial patterning of exocytosis is impaired in T2D β-cells

In addition to its ability to initiate β-cell action potential firing, glucose signaling amplifies depolarization-induced insulin secretion and β-cell exocytosis (11, 41). Glucose, but not direct depolarization with KCl, can diminish membrane granule turnover in mouse β-cells (42). We stimulated β-cells with depolarizing KCl at either 1- or 5-mM glucose. Temporal analysis reveals that exocytosis is impaired in T2D β-cells under both conditions (**Fig 2A, B**). At 1 mM glucose, the spatial uniformity of fusion events in ND β-cells was not different than that predicted by random simulation, but this increased in the presence of 5 mM glucose (**Fig 2C**). Examining β-cells with equivalent rates of exocytosis in ND and T2D (**Fig 2D**, *dashed box* and *inset*), KCl-stimulated exocytosis at 5 mM glucose showed an increased proportion of fusion events at 'hot spots' (**Fig 2E**), along with an increased density of these sites (**Fig 2F**), effects that are blunted in β-cells of donors with T2D (**Fig 2E-F**).

Observation of fusion occurring near sites of concurrent or recent membrane-resident granules

Insulin granule docking is a critical glucose-dependent step in insulin secretion, and is dysregulated in T2D (12). Considering that glucose-stimulation recruits and KCl-stimulation depletes docking granules (43), together with our observation that glucose increases the proportion and density of 'hot spots', we hypothesized that membrane-associated granules may mark sites where repeated exocytosis occurs. Many fusion events throughout our recordings

overlap with sites of membrane-resident granules observed at the initiation of imaging (**Fig 3A; Suppl Movie 3**). As illustrated in **Fig 3B** (and **Suppl Movie 4**) we observe fusion events that happen both around pre-docked granules and, later in the same recording, at this site after the pre-docked granule had fused. We have excluded events from this analysis that occur within very rapid (<1 s) succession directly overlaid with a docked granule (**Fig 3C**) since this may represent 'flickering' or 'kiss and run' of an individual granule.

Sequential fusion events are less often observed in T2D β-cells, which is dominated by individual events (**Fig 3D**). We find in ND β-cells (5 mM glucose) that 67.4% of fusion events occur at sites marked by membrane-associated granules present within the first frame of the recording, including the fusion of that docked granule itself, while only 55.2% of exocytosis in T2D β-cells occurs near such sites (**Fig 3E**). Importantly, the overall density of membrane-associated granules is decreased 35.8% in T2D β-cells (**Fig 3E**), which is consistent with a previous report (12).

The density of membrane resident granules, and fusion 'hot spots', is controlled by Kv2.1

We demonstrated previously in insulinoma cells that the ability of the Kv2.1 voltage-gated K^+ channel to form multi-channel membrane resident clusters controls the density of membrane-associated granules (32) and that fusion events occur on the periphery of Kv2.1 clusters (20). Knockdown of Kv2.1 expression in human β-cells (**Fig 4A**) reduces the density of pre-docked secretory granules in human β-cells (**Fig 4B**) and the frequency of fusion events observed at 5 mM glucose (following a 1 mM glucose preincubation) (**Fig 4C**) but not the overall proportion of those events that occur near the pre-docked granules (**Fig 4D**). Calculation of Uniform Index values demonstrates significant spatial compartmentalization that is modestly, but significantly, reduced following Kv2.1 knockdown (**Fig 4E**). Similar results are observed upon analysis of a subset of cells (*dashed box*, **Fig 4F**) with similar levels of exocytosis (**Fig 4G**), where the proportion of exocytotic events occurring at hot spots was unchanged (**Fig 4H**), but the overall density of these was decreased (**Fig 4I**).

The formation of multi-channel clusters is required for the facilitation of β-cell exocytosis by Kv2.1 (20, 32). Expression of a C-terminal truncated channel (Kv2.1-ΔC318) shown by us and others to be clustering-deficient (32, 44) in ND β-cells reduced the uniformity of fusion events

(**Fig 5A**). In a subset of ND cells with equivalent exocytosis (**Fig 5B**, *dashed box*), up-regulation of wild-type Kv2.1 has only a modest effect if any on the spatial organization of fusion events, while the Kv2.1-ΔC318 decreases the spatial uniformity of events in ND β-cells (**Fig 5C, D**). In T2D β-cells, up-regulation of the wild-type channel restored the spatial uniformity of events (**Fig 5E-H**), and this is statistically significant compared to the mCherry control group. These results suggest in part that Kv2.1 expression level and formation of multi-channel clusters controls the density of membrane-resident granules, but with little impact on whether fusion events happen at these spatially localized sites. We find that Kv2.1 clusters can recruit 30.0% more insulin granules and increase exocytosis around these by 42.4% compared to the mCherry control group in ND donors (**Fig 5I**). Similarly, in T2D donors, Kv2.1 clusters can increase membrane-associated granules by 37.5% and increase fusion events around these by 50% while the cluster-deficient mutant has no effect on exocytosis spatial patterning (**Fig 5J**).

SUMOylation sites on Kv2.1 determine the proportion of fusion events occurring in hot spots

The expression and clustering of Kv2.1 contributes to the spatial coordination of fusion events secondary to the control of membrane-resident granule density. However, we (45) and others (36) have shown that Kv2.1 is regulated by post-translational SUMOylation. The most well established SUMOylation site on the channel is located at lysine 470 (36) within a syntaxin 1A binding domain of the C-terminus (46) previously shown to have a role in β-cell exocytosis (33). A second SUMOylation motif, at lysine 145 within a potential SNAP-25 binding domain in the N-terminus (47), is however more highly conserved across species (**Fig 6A**) and homologous to a demonstrated SUMOylation site in other Kv channels, such as Kv1.1, Kv1.2 and Kv1.5 (48) (**Fig 6B**). Mutation of K145 does not appear to alter Kv2.1 currents (36), which we confirm (**Fig 6C, D**). However, loss of the K145 SUMOylation site (Kv2.1-K145R) blunts the suppressive effect of SUMO1 on exocytosis in insulinoma cells (**Fig 6E-H**) and when combined with abolishing the K479 SUMOylation site (Kv2.1-K145/470R) completely prevents SUMO1-dependent suppression of exocytosis (**Fig 6E,F**).

In human β-cells from donors without diabetes, increasing SUMO1 blunts exocytosis (38) in concert with impaired spatial compartmentalization of fusion events (**Fig 7A,B**). Loss of Kv2.1

SUMOylation sites in the Kv2.1-K145/470R double mutant prevents this (**Fig 7C,D**). In cells with equivalent rates of exocytosis (**Fig 7E**, *dashed box*), we find that SUMO1 reduces the uniformity of events such that the uniform index is no longer different from random simulations and this is completely prevented in the Kv2.1-K145/470R group (**Fig 7F**). Finally, in these cells, SUMOylation of Kv2.1 reduces the proportion of fusion events occurring within 'hot spots' (**Fig 7G**) with only minimal impact on their total density (**Fig 7H**).

DISCUSSION

The regulated exocytosis of insulin from human pancreatic β-cells is impaired in T2D. Indeed, reduced exocytotic function is observed even in β-cells of human donors with genetic risk for T2D (10). Several factors likely contribute to this lower exocytotic responsiveness, including reduced SNARE expression (8), a loss of regulatory metabolic signals (11), impaired microtubule (49) or actin (50) regulation of granule access to the membrane, and the uncoupling of granule fusion from sites of Ca^{2+} entry. The latter has been described in models of free fatty acid culture (27), high fat fed mice (28), and in β-cells from human T2D donors (18). Recently, the glucose-dependent recruitment of granules to docking sites was shown to be a limiting step in insulin secretion which is disturbed in T2D (12). The spatial organization of events at the plasma membrane, such as the localization of integrin signals (15) or the clustering of Ca^{2+} channels (18), are important determinants of regulated insulin secretion. However, little is understood about the control of the spatial patterning of fusion events and the relevance of this to human T2D.

An insulin secretory deficit, including a reduced responsiveness to glucose, is an important determinant of T2D development and progression (51). While impaired islet mass may contribute to reduced insulin secretion in T2D, at least later in the disease (5), the contribution of reduced islet insulin content versus impaired secretory responses early in T2D progression is less well recognized. Although insulin content has been shown to be decreased in T2D human islets by us (40) and others (39), in the present data-set we observed impaired insulin secretory responses without an obvious decrease in insulin content (**Fig 1**). This is likely due to the relatively short duration of T2D in this cohort (6.7 +/-1.9 years) where only 5/18 donors had reported disease duration of 10 years or more. Of the three T2D donors with no information on disease duration,

two appeared well-controlled (HbA1c 5.6, 6.2) and one was controlled with diet only. While reported disease duration needs to be treated with caution, we show that impairment in insulin secretion can occur independent of a reduced islet insulin content. Indeed, cell-autonomous reductions in insulin exocytosis from human T2D β-cells have been reported by us (11, 32) and others (12). We confirm this in both electrophysiological and imaging assays of granule fusion, and provide evidence that the impaired secretion of insulin from these donors results in part from a reduced glucose-dependent facilitation of exocytosis (**Fig 1C,D** and **Fig 2A,B**).

While more is known about the distal granule fusion apparatus, that is granule docking and fusion on the Ca^{2+} channel, less is known about the precise architecture by which granules approaching the plasma membrane actually get to the fusion sites. Glucose-dependent granule docking (12) and the localization of granule fusion to sites of Ca^{2+} entry (18, 27, 28) are disrupted in T2D. Previous studies have suggested both directional control of insulin release towards the vasculature in situ (13-16) and the existence of repetitive release sites (19-23). We therefore examined the spatial organization of fusion across the cell surface in human β-cells and find significant patterning of events. Moreover, the spatial and temporal analyses of insulin granule release in isolated intact human islets reveals that exocytosis is localized to preferential release sites, and prolonged stimulation with high glucose increases this compartmentalization (13). This could be explained by glucose-dependent recruitment of insulin granules to defined sites on the cell membrane, and we do find that most fusion events (~65% in ND β-cells) result from release of granules at sites marked by previously or concurrently docked granules (**Fig 3**), and consistent with the relationship between glucose-dependent granule recruitment and spatial organization – we find that elevated glucose is required for the spatial patterning of fusion events (**Fig 2**) and the facilitation of β-cell exocytotic responses (11) (**Fig 1B**). The observation that membrane-docked granules mark 'hot spots' in β-cells suggests that the reduced organization of fusion events in T2D β-cells could be secondary to impaired glucose-dependent granule docking. In T2D donors reduced glucose-dependent docking is suggested as a major upstream defect (12), and we also report a reduced density of membrane-associated granules in T2D β-cells (**Fig 3E**).

SNARE proteins and ion channels are compartmentalized across the cell membrane, in complexes which are generally thought to facilitate efficient exocytosis. Previously, we reported

that Kv2.1 in pancreatic β-cells co-localizes with docking granules (20, 32). The ability of Kv2.1 to directly facilitate exocytosis, independent of its electrical function (35), requires the formation of multi-channel clusters (32). Indeed, we recently demonstrated that fusion events in insulinoma cells occur adjacent to Kv2.1 clusters (20) and suggested that these sites act as 'reservoirs ' for the provision of release-competent granules. This role is supported by our observation that depletion or over-expression of Kv2.1 reduces or increases, respectively, the density of membrane-resident granules and consequently the density of fusion 'hot spots' (**Figs 4, 5**). This has a less prominent effect however on the overall proportion of total fusion events occurring in spatially restricted regions (i.e. the 'hot spots ratio'), suggesting that while Kv2.1 contributes to setting the number of 'hot spots' another mechanism is involved in determining or direction fusion at these sites.

SUMOylation is an important regulatory mechanism for membrane proteins. Kv2.1 can by SUMOylated (36, 45), and we find an important functional effect of manipulating SUMOylation sites in both the N- and C-terminus of the channel. The N-terminal SUMOylation site is less well established and has no apparent impact on the biophysical function of K^+ conductance, in line with a previous report (36). We do however find that this is more highly conserved between species and amongst Kv isoforms (**Fig 6**). This site in Kv1.5 has a demonstrated function in SUMO-control of the channel (48) and here we show that mutation of the consensus lysine residue (K145) reduces the inhibitory effect of SUMOylation on exocytosis in concert with the C-terminal site (K470). This has only minimal impact on the density of 'hot spots' (**Fig 7H**), but instead controls the proportion of events that occur at these sites (**Fig 7H**). It seems that Kv2.1 SUMOylation, which occurs at sites of syntaxin-1A/-3 (52) and SNAP-25 (47) binding might not alter the ability for granules to be recruited to the 'reservoir', but instead impacts the transfer of granules to the actual fusion sites. This, and the roles in sequential insulin granule fusion for Munc18b (21) and syntaxin-3 (53), which bind the channel (20), suggest that the likely mechanism for the sequential fusion involves Kv2.1 interactions with an alternate SNARE complex.

In summary, we demonstrate a glucose-dependent spatiotemporal compartmentalization of insulin granule fusion events in human β-cells. This contributes to the amplification of insulin exocytosis by glucose, and is perturbed in T2D. The voltage-gated K^+ channel Kv2.1 plays a

structural role in this process, likely as a component of a complex serving as a 'reservoir' of granules for future fusion. Kv2.1 helps to set the density of these sites, while deSUMOylation of the channel supports the progression of granules to a fusion-competent state.

METHODS

Human islets and cell culture. Human islets were isolated at the Alberta Diabetes Institute IsletCore (www.bcell.org/isletcore.html) according to procedures deposited in the protocols.io repository (54). A total of 62 donors with no-diabetes (ND; **Suppl Table 1**) and 18 donors with type 2 diabetes (T2D; **Suppl Table 2**) were examined in this study. The presence of T2D was determined by clinical reporting at the time of organ procurement, or an HbA1c >6.5% measured from blood tubes provided with the shipped organ. Prior to experiments, islets were cultured in low-glucose (5.5 mM) DMEM with L-glutamine, 110 mg/l sodium pyruvate, 10% FBS, and 100 U/ml penicillin/streptomycin. All human islet studies were approved by the Human Research Ethics Board (Pro00013094; Pro00001754) at the University of Alberta and all families of organ donors provided written informed consent.

Human embryonic kidney (HEK) 293 cells were cultured in DMEM with 20 mM glucose, 10% FBS, 100 units/mL penicillin, and 100 mg/mL streptomycin at 37°C and 5% CO_2. The glucose responsive INS 832/13 insulinoma cell line (55) was cultured in RPMI-1640 with 11.1 mM glucose, 10% FBS, 10 mM HEPES, 0.29 mg/ml L-glutamine, 1 mM sodium pyruvate, 50 µM 2-mercaptoethanol, 100 U/ ml penicillin, and 100 mg/mL streptomycin.

Adenoviruses, constructs, and treatments. Human pancreatic islets were dissociated using Cell Dissociation Buffer enzyme-free, Hanks' Balanced Salt Solution (ThermoFisher Scientific. Burlington, ON). Isolated human pancreatic β-cells were infected with adenovirus expressing NPY-EGFP and further cultured for 24-36 h before imaging. We confirmed the localization of NPY-EGFP to insulin granules by immunostaining. Adeno-NPY-eGFP infected human pancreatic β-cells were transfected for 36-48 h with the expression plasmids as outlined for each experiment using Lipofectamine 2000 (Life Technologies, Burlington, ON).

The cDNA encoding wild type rat Kv2.1 or the truncated Kv2.1-ΔC318 (Kv2.1 Glu536_Ile853 del) was amplified by PCR using a pcDNA3.1-Kv2.1 plasmid (45) as a template, and inserted between BsrG-I and Xho-I site of Cherry-LacRep plasmid (from Mirek Dundr: Addgene plasmid #18985) by Gibson Assembly to make mCherry-Kv2.1-WT and mCherry-Kv2.1-ΔC318.

To generate Myc-tagged Kv2.1 plasmids, the cDNA encoding 5xMyc was inserted between Nhe-I and BsrG-I sites of the mCherry-Kv2.1-WT and mCherry-Kv2.1-ΔC318 expression vector by Gibson Assembly. To generate the mutation of SUMOylation sites in Kv2.1, site-directed mutagenesis was performed in a Myc-tagged Kv2.1-WT expression vector to introduce the mutation from lysine to arginine at the position K145, K470 and K145/470. All mutations were confirmed by Sanger DNA sequencing.

The full-size human SUMO1 cDNA, IRES DNA and mCherry cDNA were prepared by PCR using pEYFP SUMO-1 plasmid (from Mary Dasso: Addgene plasmid #13380), pWPI plasmid (from Didier Trono: Addgene plasmid #12254) or Cherry-LacRep plasmid as template, respectively. The pCMV-hSUMO1-IRES-mCherry plasmid was constructed by inserting the cDNA/DNA of Human SUMO1, IRES and mCherry, in this sequence, between Nhe-I and BamH-I sites of Cherry-LacRep plasmid by Gibson assembly. Negative control plasmid, pIRES-mCherry, was prepared in the same manner but without Human SUMO1 cDNA.

Finally, knockdown of KCNB1 expression in human cells was carried out using a mixture of 4 siRNA duplexes (Qiagen; Cat#: S100070777, S100070791, S100070798, S103065930) in which each recognizes different regions of the human KCNB1 gene. Knockdown of KCNB1 was confirmed by qPCR using Taqman expression assays (Assay ID Hs00270657_m1 for KCNB1, Hs00191116_m1 for KCNB2, Applied Biosystems/Thermo Fisher Scientific, MA USA).

Insulin secretion and electrophysiology. The insulin secretion measurements are detailed in the protocol deposited to protocols.io (56). Glucose concentrations were 1 and 10 mM, after which insulin content was extracted with acid/ethanol. The samples were stored at −20°C and assayed by chemiluminescent immunoassay (STELLUX, Alpco Diagnostics) or electro-chemiluminescent immunoassay (Huaman Insulin Kit, Meso Scale Diagnostics). Experiments were performed in triplicate, and the averaged values were used for analyses. Patch-clamp measurement of Kv

currents and exocytotic responses in single HEK293, INS 832/13 or human β-cells, the latter identified by positive insulin immunostaining following the experiment, were performed at 32-35°C as described (33) using a HEKA EPC10 amplifier and PatchMaster Software (HEKA, Lambrecht, Germany).

TIRFM Imaging. All TIRF imaging used a Cell-TIRF motorized system (IX83P2ZF, Olympus Canada) with a 100×/1.49 NA TIRFM objective, a Photometrics Evolve 512 camera (Photometrics), and Metamorph Imaging software (Molecular Devices). Excitation was at 491 nm (LAS-491-50) and 561 nm (LAS-561-50, Olympus, Germany) with a quad filter passing through a major dichroic and band pass filter (405/488/561/640, Chroma Technology, Bellows Falls, VT). Penetration depth was set to 105 nm, calculated using existing angle of the laser and assuming a refractive index of 1.37. Emission was collected through bandpass filters of 525/25 nm and 605/26 nm for excitations of 488 and 561 nm, respectively. Images were acquired sequentially with single laser excitation to minimize potential bleed-through.

Live-cell acquisition was 5-Hz with a 200 ms exposure at 35°C. Before acquisition, cells were pre-incubated (30 mins) in bath containing (in mM) 138 NaCl, 5.6 KCl, 1.2 $MgCl_2$, 2.6 $CaCl_2$, 5 $NaHCO_3$, 1 glucose and 5 HEPES (pH 7.4 with NaOH) and then exposed to 5 mM glucose upon recording. In glucose-stimulation experiments the buffer contained 16.7 mM glucose. For KCl stimulation, the buffer instead contained 30 mM KCl which replaced an equimolar amount of NaCl. Fusion events, indicated by abrupt brightening (ratio of peak fluorescence to background >1.3) and then disappearance of NPY-EGFP fluorescence, were selected and analyzed with a compiled MATLAB (MathWorks) based analysis software (19) within the membrane area (the authors kindly provided their software). Docked granules were detected using a "local maxima" or a weighted centroid method (within a range of 4 × 4 pixels, 0.6328 × 0.6328 μm) (19). Exocytosis events occurring around docking granule were manually selected following overlay of fusion events with identified sites of membrane-resident granules at the start of recordings.

Spatial analysis was performed in MATLAB, 2018a (MathWorks). Voronoi polygons were used to separate each fusion event. Random simulation was with the same number of fusion events and the same cell boundaries. The 'observation' uniform index (19) was calculated as the

standard deviation of the fusion area divided by the mean of the fusion area. The 'simulation' uniform index was calculated similarly following a random distribution of events. Exocytosis hot spots, recognized by MATLAB, was run with a threshold value of 0.6328 μm, which is <4 pixels and represents the minimum resolvable distance to distinguish two granule fusion sites in our system. The 'hot spot ratio (%)' was calculated as the number of fusion events occurring at hot spots divided by the total fusion events and multiplied by 100. The 'hot spot density (#/100 μm^2) was calculated as the number of hot spots normalized to cell footprint area. Hot spots visualization heat maps were generated through interpolation (MATLAB 'v4' interpolation method) using number of events as the third dimension on a 1-pixel resolution grid.

Statistical analysis. Data analysis was performed using Fit Master (HEKA Electronik), Origin Lab (v7.0) and GraphPad Prism (v6.0c). All data are shown as the mean ± SEM. Statistical outliers were identified and removed by an unbiased ROUT (robust regression followed by outlier identification) test. Comparison of multiple groups was by ANOVA and Bonferroni post-hoc test. When comparing two means only, data were analyzed by the 2-tailed Student's t test. A p-value less than 0.05 was considered significant.

Acknowledgments

We wish to thank Dr. Yongdeng Zhang (Yale University) for providing the computer-assisted analysis software and advice on data analysis. The authors thank the Human Organ Procurement and Exchange (HOPE) and Trillium Gift of Life Network (TGLN) programs for their efforts in procuring pancreas for research. The authors also thank Mr. James Lyon and Mrs. Nancy Smith (Alberta Diabetes Institute IsletCore, University of Alberta) for work isolating human research islets. Human research islet isolations were supported by the Alberta Diabetes Foundation and the University of Alberta. Research was funded by a Foundation Grant from the Canadian Institutes of Health Research (CIHR: 148451) to PEM.

Author Contributions

JF, JMG, XD, GP, KS, AFS, AB, RJK, DGA, and JEMF researched data; JF, HYG and PEM conceived the study; JF and PEM wrote the manuscript; All authors edited and approved this version.

Conflict of Interest

The authors declare no conflict of interest.

References

1. Tokarz VL, MacDonald PE, Klip A. The cell biology of systemic insulin function. *J. Cell Biol.* 2018;217(7):2273-2289.

2. Kahn SE, Cooper ME, Del Prato S. Pathophysiology and treatment of type 2 diabetes: perspectives on the past, present, and future. *Lancet* 2014;383(9922):1068–1083.

3. Schwartz SS et al. The time is right for a new classification system for diabetes: Rationale and implications of the β-cell-centric classification schema. *Diabetes Care* 2016;39(2):179–186.

4. Ha J, Satin LS, Sherman AS. A mathematical model of the pathogenesis, prevention, and reversal of type 2 diabetes. *Endocrinology* 2016;157(2):624–635.

5. Butler AE et al. Beta-cell deficit and increased beta-cell apoptosis in humans with type 2 diabetes. *Diabetes* 2003;52(1):102–110.

6. Del Guerra S et al. Functional and molecular defects of pancreatic islets in human type 2 diabetes. *Diabetes* 2005;54(3):727–735.

7. Deng S et al. Structural and functional abnormalities in the islets isolated from type 2 diabetic subjects. *Diabetes* 2004;53(3):624–632.

8. Ostenson C-G, Gaisano H, Sheu L, Tibell A, Bartfai T. Impaired gene and protein expression of exocytotic soluble N-ethylmaleimide attachment protein receptor complex proteins in pancreatic islets of type 2 diabetic patients. *Diabetes* 2006;55(2):435–440.

9. Andersson SA et al. Reduced insulin secretion correlates with decreased expression of exocytotic genes in pancreatic islets from patients with type 2 diabetes. *Mol. Cell. Endocrinol.* 2012;364(1-2):36–45.

10. Rosengren AH et al. Reduced insulin exocytosis in human pancreatic β-cells with gene variants linked to type 2 diabetes. *Diabetes* 2012;61(7):1726–1733.

11. Ferdaoussi M et al. Isocitrate-to-SENP1 signaling amplifies insulin secretion and rescues dysfunctional β cells. *J. Clin. Invest.* 2015;125(10):3847–3860.

12. Gandasi NR et al. Glucose-Dependent Granule Docking Limits Insulin Secretion and Is Decreased in Human Type 2 Diabetes. *Cell Metab.* 2018;27(2):470–478.e4.

13. Almaça J et al. Spatial and temporal coordination of insulin granule exocytosis in intact human pancreatic islets. *Diabetologia* 2015;58(12):2810–2818.

14. Low JT et al. Insulin secretion from beta cells in intact mouse islets is targeted towards the vasculature. *Diabetologia* 2014;57(8):1655–1663.

15. Gan WJ et al. Local integrin activation in pancreatic β cells targets insulin secretion to the vasculature. *Cell Rep* 2018;24(11):2819–2826.e3.

16. Ohara-Imaizumi M et al. ELKS/Voltage-dependent Ca^{2+} channel-β subunit module regulates polarized Ca^{2+} influx in pancreatic β cells. *Cell Rep* 2019;26(5):1213–1226.e7.

17. Yasuda T et al. Rim2alpha determines docking and priming states in insulin granule exocytosis. *Cell Metab.* 2010;12(2):117–129.

18. Gandasi NR et al. Ca^{2+} channel clustering with insulin-containing granules is disturbed in type 2 diabetes. *J. Clin. Invest.* 2017;127(6):2353–2364.

19. Yuan T, Lu J, Zhang J, Zhang Y, Chen L. Spatiotemporal detection and analysis of exocytosis reveal fusion “hot spots” organized by the cytoskeleton in endocrine cells. *Biophys. J.* 2015;108(2):251–260.

20. Greitzer-Antes D et al. Kv2.1 clusters on β-cell plasma membrane act as reservoirs that replenish pools of newcomer insulin granule through their interaction with syntaxin-3. *J. Biol. Chem.* 2018;293(18):6893–6904.

21. Lam PPL et al. Munc18b is a major mediator of insulin exocytosis in rat pancreatic β-cells. *Diabetes* 2013;62(7):2416–2428.

22. Takahashi N, Kishimoto T, Nemoto T, Kadowaki T, Kasai H. Fusion pore dynamics and insulin granule exocytosis in the pancreatic islet. *Science* 2002;297(5585):1349–1352.

23. Kwan EP, Gaisano HY. Glucagon-like peptide 1 regulates sequential and compound exocytosis in pancreatic islet beta-cells. *Diabetes* 2005;54(9):2734–2743.

24. Barg S, Knowles MK, Chen X, Midorikawa M, Almers W. Syntaxin clusters assemble reversibly at sites of secretory granules in live cells. *Proc. Natl. Acad. Sci. U.S.A.* 2010;107(48):20804–20809.

25. Knowles MK et al. Single secretory granules of live cells recruit syntaxin-1 and synaptosomal associated protein 25 (SNAP-25) in large copy numbers. *Proc. Natl. Acad. Sci. U.S.A.* 2010;107(48):20810–20815.

26. Ohara-Imaizumi M et al. Correlation of syntaxin-1 and SNAP-25 clusters with docking and fusion of insulin granules analysed by total internal reflection fluorescence microscopy. *Diabetologia* 2004;47(12):2200–2207.

27. Hoppa MB et al. Chronic palmitate exposure inhibits insulin secretion by dissociation of Ca^{2+} channels from secretory granules. *Cell Metab.* 2009;10(6):455–465.

28. Collins SC et al. Progression of diet-induced diabetes in C57BL6J mice involves functional dissociation of Ca^{2+} channels from secretory vesicles. *Diabetes* 2010;59(5):1192–1201.

29. Rorsman P, Ashcroft FM. Pancreatic β-cell electrical activity and insulin secretion: Of mice and men. *Physiol. Rev.* 2018;98(1):117–214.

30. Braun M et al. Voltage-gated ion channels in human pancreatic beta-cells: electrophysiological characterization and role in insulin secretion. *Diabetes* 2008;57(6):1618–1628.

31. O'Connell KMS, Tamkun MM. Targeting of voltage-gated potassium channel isoforms to distinct cell surface microdomains. *J. Cell. Sci.* 2005;118(Pt 10):2155–2166.

32. Fu J et al. Kv2.1 clustering contributes to insulin exocytosis and rescues human β-cell dysfunction. *Diabetes* 2017;66(7):1890–1900.

33. Dai XQ et al. The voltage-dependent potassium channel subunit Kv2.1 regulates insulin secretion from rodent and human islets independently of its electrical function. *Diabetologia* 2012;55(6):1709–1720.

34. Leung YM, Kwan EP, Ng B, Kang Y, Gaisano HY. SNAREing voltage-gated K^+ and ATP-sensitive K+ channels: tuning beta-cell excitability with syntaxin-1A and other exocytotic proteins. *Endocr. Rev.* 2007;28(6):653–663.

35. Singer-Lahat D et al. K^+ channel facilitation of exocytosis by dynamic interaction with syntaxin. *J. Neurosci.* 2007;27(7):1651–1658.

36. Plant LD, Dowdell EJ, Dementieva IS, Marks JD, Goldstein SAN. SUMO modification of cell surface Kv2.1 potassium channels regulates the activity of rat hippocampal neurons. *J. Gen. Physiol.* 2011;137(5):441–454.

37. MacDonald PE. A post-translational balancing act: the good and the bad of SUMOylation in pancreatic islets. *Diabetologia* 2018;61(4):775–779.

38. Dai X-Q et al. SUMOylation regulates insulin exocytosis downstream of secretory granule docking in rodents and humans. *Diabetes* 2011;60(3):838–847.

39. Marchetti P et al. Pancreatic islets from type 2 diabetic patients have functional defects and increased apoptosis that are ameliorated by metformin. *J. Clin. Endocrinol. Metab.* 2004;89(11):5535–5541.

40. Lyon J et al. Research-focused isolation of human islets from donors with and without diabetes at the Alberta Diabetes Institute IsletCore. *Endocrinology* 2016;157(2):560–569.

41. Gembal M, Gilon P, Henquin JC. Evidence that glucose can control insulin release independently from its action on ATP-sensitive K^+ channels in mouse B cells. *J. Clin. Invest.* 1992;89(4):1288–1295.

42. Brüning D, Reckers K, Drain P, Rustenbeck I. Glucose but not KCl diminishes submembrane granule turnover in mouse beta-cells. *J. Mol. Endocrinol.* 2017;59(3):311–324.

43. Ohara-Imaizumi M, Nakamichi Y, Tanaka T, Ishida H, Nagamatsu S. Imaging exocytosis of single insulin secretory granules with evanescent wave microscopy: distinct behavior of granule motion in biphasic insulin release. *J. Biol. Chem.* 2002;277(6):3805–3808.

44. O'Connell KMS, Rolig AS, Whitesell JD, Tamkun MM. Kv2.1 potassium channels are retained within dynamic cell surface microdomains that are defined by a perimeter fence. *J. Neurosci.* 2006;26(38):9609–9618.

45. Dai X-Q, Kolic J, Marchi P, Sipione S, MacDonald PE. SUMOylation regulates Kv2.1 and modulates pancreatic beta-cell excitability. *J. Cell. Sci.* 2009;122(Pt 6):775–779.

46. Leung YM et al. Syntaxin 1A binds to the cytoplasmic C terminus of Kv2.1 to regulate channel gating and trafficking. *J. Biol. Chem.* 2003;278(19):17532–17538.

47. MacDonald PE et al. Synaptosome-associated protein of 25 kilodaltons modulates Kv2.1 voltage-dependent K^+ channels in neuroendocrine islet beta-cells through an interaction with the channel N terminus. *Mol. Endocrinol.* 2002;16(11):2452–2461.

48. Benson MD et al. SUMO modification regulates inactivation of the voltage-gated potassium channel Kv1.5. *Proc. Natl. Acad. Sci. U.S.A.* 2007;104(6):1805–1810.

49. Zhu X et al. Microtubules negatively regulate insulin secretion in pancreatic β cells. *Dev. Cell* 2015;34(6):656–668.

50. Veluthakal R et al. Restoration of glucose-stimulated Cdc42-Pak1 activation and insulin secretion by a selective Epac activator in type 2 diabetic human islets. *Diabetes* 2018;67(10):1999–2011.

51. Ferrannini E et al. β-cell function in subjects spanning the range from normal glucose tolerance to overt diabetes: A new analysis. *J. Clin. Endocrinol. Metab.* 2005;90(1):493–500.

52. Leung YM et al. Syntaxin 1A binds to the cytoplasmic C terminus of Kv2.1 to regulate channel gating and trafficking. *J. Biol. Chem.* 2003;278(19):17532–17538.

53. Zhu D et al. Syntaxin-3 regulates newcomer insulin granule exocytosis and compound fusion in pancreatic beta cells. *Diabetologia* 2013;56(2):359–369.

54. Lyon J et al. Isolation of Human Pancreatic Islets of Langerhans for Research v2 (protocols.io.xgsfjwe). *protocols.io*; doi:10.17504/protocols.io.xgsfjwe

55. Hohmeier HE et al. Isolation of INS-1-derived cell lines with robust ATP-sensitive K^+ channel-dependent and -independent glucose-stimulated insulin secretion. *Diabetes* 2000;49(3):424–430.

56. Spigelman A. Static Glucose-stimulated Insulin Secretion (GSIS) Protocol - Human Islets v2 (protocols.io.wy4ffyw). *protocols.io*; doi:10.17504/protocols.io.wy4ffyw

Figure Legends

Figure 1. Impaired β-cell exocytosis and spatial compartmentalization of exocytosis in T2D.

A) Compared to islets of donors with no diabetes (ND; n=62), glucose-stimulated insulin secretion is impaired from islets of donors with type 2 diabetes (T2D; n=18). **B)** In these donors (avg. 6.7 years duration) islet insulin content is not different. **C-D)** Cumulative distribution of exocytotic responses of β-cells from the same donors, measured by patch-clamp electrophysiology. Glucose (10 mM; *red*) amplifies the exocytotic responses of ND β-cells (**C**; n=688 cells) but not T2D β-cells (**D**; n=169 cells). **E)** Fusion events (*red circles*) observed by live-cell TIRF microscopy at 5 mM glucose in ND β-cells, a heatmap of fusion event density, and Voronoi diagram used to separate exocytosis sites. **F)** Representative recordings from the areas indicated in panel E. **G)** The non-random nature of fusion events in ND β-cells is demonstrated by spatial K-function calculation (*red line*) greater than the simulated (*dashed lines*) maximum. **H-J)** The same as panels E-G, but in a T2D β-cell, where events appear more randomly distributed. **K)** Exocytosis measured by patch-clamp in a sub-set of donors at 5 mM glucose, demonstrates impaired function in T2D (n=12 and 16 cells from ND 3 and 3 T2D donors). **L)** Accumulated fusion events monitored by TIRF microscopy of β-cells, also at 5 mM glucose (n=16 and 26 cells from 5 and 6 donors). **M)** Uniform index of events from panel L calculated (*black*) from Voronoi polygon areas and compared with random simulations (*grey*). **N)** Scatter plot of total fusion events versus the ratio at which these occur within clusters. A subset of cells (*dashed box*) with equivalent exocytosis (*inset*) were selected for further analysis. **O)** The proportion of events occurring in spatially defined clusters, and; **P)** The density of these clusters. *P<0.05; **p<0.01; and ***p<0.001. Scale bars 5 μm.

Figure 2. Spatial organization of fusion events is upregulated by glucose.

A-B) Accumulated fusion events monitored by TIRF microscopy of ND β-cells (*black circles*) and T2D β-cells (*open circles*) in response to KCl at 1 mM (**A**; n=7 and 8 cells from 6 and 3 donors) and 5 mM glucose (**B**; n=9 and 9 cells from 6 and 3 donors). **C)** The uniform index is increased at 5 mM glucose in the ND (*closed symbols*), but not T2D (*open symbols*), β-cells. **D)** Scatter plot showing total fusion events versus the proportion of events in spatially restricted clusters. Cells with similar exocytosis (*dashed box*) used for further analysis. **E-F)** The proportion

of events occurring in organized clusters (**E**) and the density of these clusters (**F**) is increased at 5 mM glucose in ND β-cells, but impaired in T2D β-cells. *p<0.05, **p<0.01, ***p<0.001.

Figure 3. Fusion occurs around sites of concurrent or recent membrane-associated granules.

A) Membrane-associated granules at the beginning of the recording are marked in green (*left*); all subsequent fusion events are shown in red (*center*); fusion events occurring at sites were membrane-localized granules were observed are shown in yellow (*right*). The latter may represent fusion of the membrane-localized granule itself (single yellow event), or of several events at a clustered site (multiple yellow events). **B)** Exocytosis occurring around a membrane-localized granule in a ND β-cell. Two events occur adjacent to a membrane-resident granule, followed by fusion of that granule itself, and then a new fusion event at the same site. **C)** Rapid flickering events before full fusion, illustrated here, are ignored in this analysis. **D)** In T2D β-cells most fusion occurred as individual, rather than as sequential, events. **E)** Quantification of the proportion of events occurring around initially membrane-localized granules (*pie charts, and bottom left*) and the initial density of membrane-resident granules (*bottom right*; n=16 and 28 cells from 3 ND and 3 T2D donors). **p<0.01, ***p<0.001. Scale bars 5 μm.

Figure 4. Kv2.1 regulates the density of membrane-resident granules and clustered fusion sites.

A) Knockdown of Kv2.1 expression by siRNA in human islet cells. **B)** The initial density of membrane-resident granules is reduced by Kv2.1 knockdown, as is; **C)** the frequency of exocytotic events. **D)** This occurs without a change in the overall proportion of fusion events occurring at sites marked by membrane-resident granules (n=30 and 30 cells from 3 donors). **E)** The spatial organization of these events is only modestly decreased. **F-I)** Examination of a sub-set of cells (**F**; *dashed box*) with similar event frequency (**G**) demonstrates that the proportion of events occurring in spatially clustered regions is unchanged by Kv2.1 knockdown (**H**) while the density of these sites is decreased (**I**). *p<0.05, **p<0.01, ***p<0.005.

Figure 5. Upregulation of Kv2.1 restores the spatial organization of fusion sites in T2D β-cells.

A) In ND β-cells, compared with the full-length channel (Kv2.1-WT) a clustering deficient mutant (Kv2.1-ΔC318) reduced the uniformity of fusion events (n=22, 26 and 24 cells from 3 donors). **B-D)** In a subset of cells with equivalent rates of exocytosis (**B**, *dashed box*) expression of Kv2.1-WT had little effect on the ratio of events within hot spots (**C**) and slightly increased their density (**D**), while Kv2.1-ΔC318 reduced the overall contribution of hot spots to exocytosis.

E-H) Same as panels A-D, but in T2D β-cells (n=12, 16 and 10 cells from 3 donors). Here, Kv2.1-WT rescued the compartmentalization of fusion events. In a sub-set of cells with similar fusion frequency (**F**; *dashed box*) the overall proportion of events occurring in these spatially restricted regions (**G**) and the density of these sites (**H**) are unchanged by WT-Kv2.1. **I-J)** Expression of Kv2.1-WT but not Kv2.1-ΔC318 in ND β-cells (**I**) or T2D β-cells (**J**) increases the density of membrane-resident granules and the proportion of fusion events at sites marked by these. *p<0.05, **p<0.01 and ***p<0.001.

Figure 6. SUMOylation sites on the Kv2.1 N- and C-termini control β-cell exocytosis.

A) Two previously demonstrated Kv2.1 SUMOylation motifs are conserved across species and between some members of the voltage-dependent K^+ channel family. **B)** Overlay of N-terminal domains of Kv2.1 and Kv1.5 showing location of demonstrated and predicted SUMOylation sites. **C-D)** Mutation of the C-terminal (K470R), but not the N-terminal (K145R), lysines to prevent SUMOylation alters Kv2.1 current kinetics when expressed in HEK293 (**C**; n=16, 7, 11, 6, 6 cells) or INS 832/13 insulinoma (**D**; n=16, 20, 27, 20, 28 cells). Western blots showing equivalent expression of these constructs is shown at the right. **E)** SUMO1 suppresses exocytosis in INS 832/13 cells expressing Kv2.1-WT (n=23, 18 cells), and this effect is reduced in cells expressing Kv2.1-K145R (n=16, 18 cells) or Kv2.1-K470R (n=27, 29 cells). Mutation of both SUMOylation sites (Kv2.1-K145/470R; n=24, 14 cells) abolished the inhibitory effect of SUMO1 on exocytosis. *p<0.05, **p<0.01 and ***p<0.001.

Figure 7. Kv2.1 SUMOylation sites regulate compartmentalization of fusion events.

A-D) Example fusion events shown individually (*left*), as density heatmaps (*middle*), or separated by Voryoni polygons (*right*) in ND β-cells expressing Kv2.1-WT alone (**A**) or with SUMO1 (**B**), and Kv2.1-K145/470R alone (**C**) or with SUMO1 (**D**). **E)** Uniformity index values calculated from Voryoni polygons show that SUMO1 reduces the compartmentalization of fusion events in cells expressing Kv2.1-WT, but not the SUMOylation-deficient mutant Kv2.1-K145/470R. (n=10, 8, 12, 12 cells from 4 donors) **F)** Scatterplot showing the relationship between proportion of events occurring within hot spots versus event frequency. A subset of cells (*dashed box*) was chosen for further analysis. **G-H)** SUMO1 reduced the proportion of events occurring at hot spots (**G**) with little impact on the overall hot spot density (**H**). *p<0.05, **p<0.01 and ***p<0.001. Scale bars 5 μm.

Figure. 1

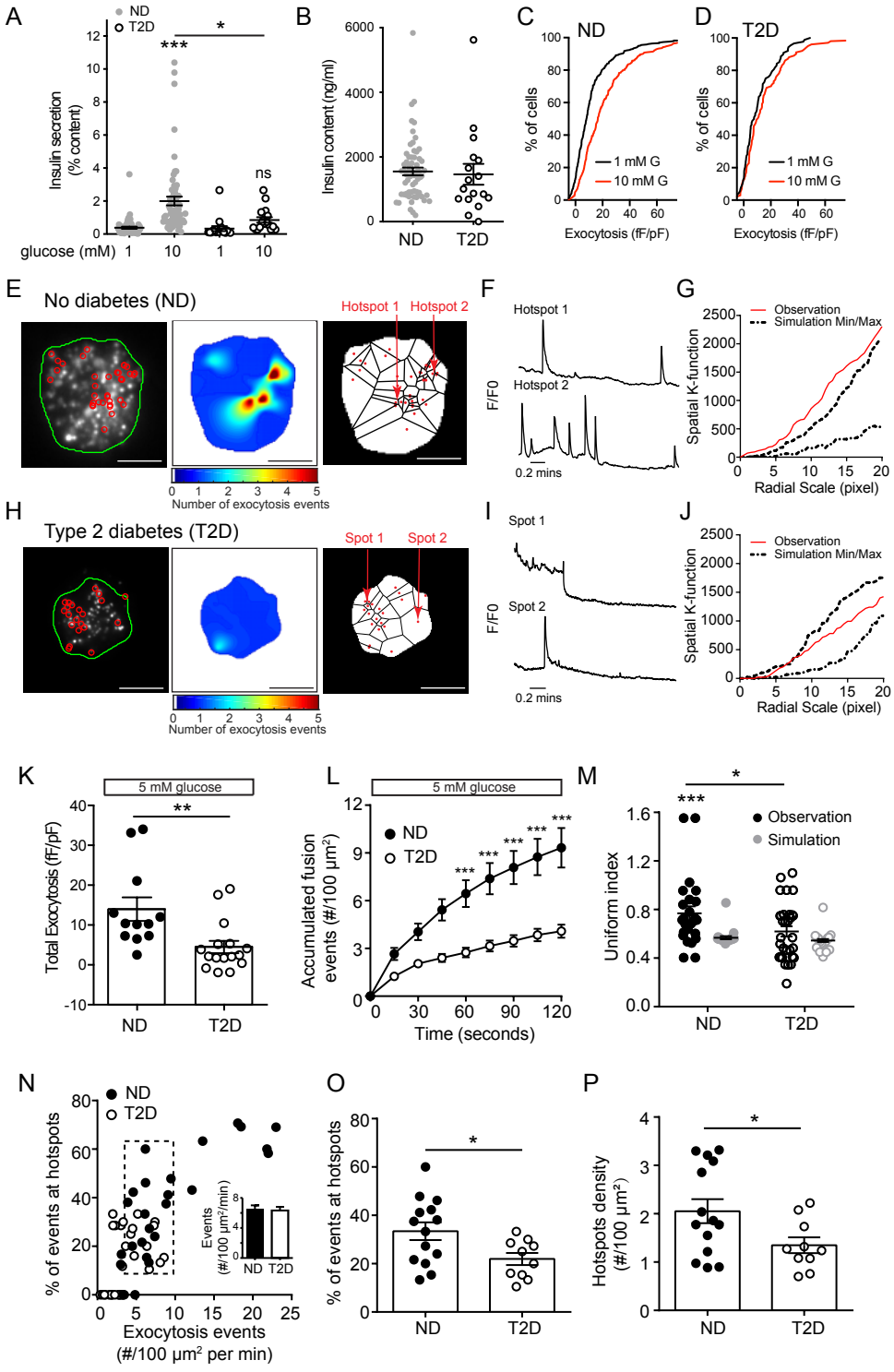

Figure. 2

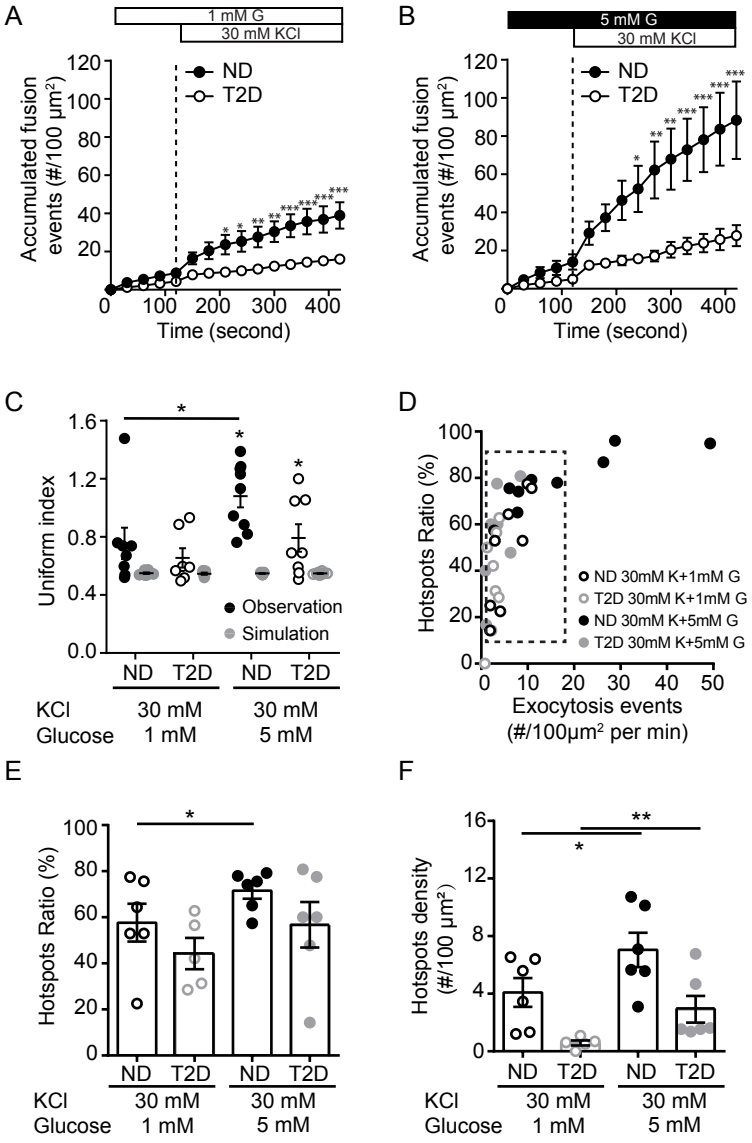

Figure. 3

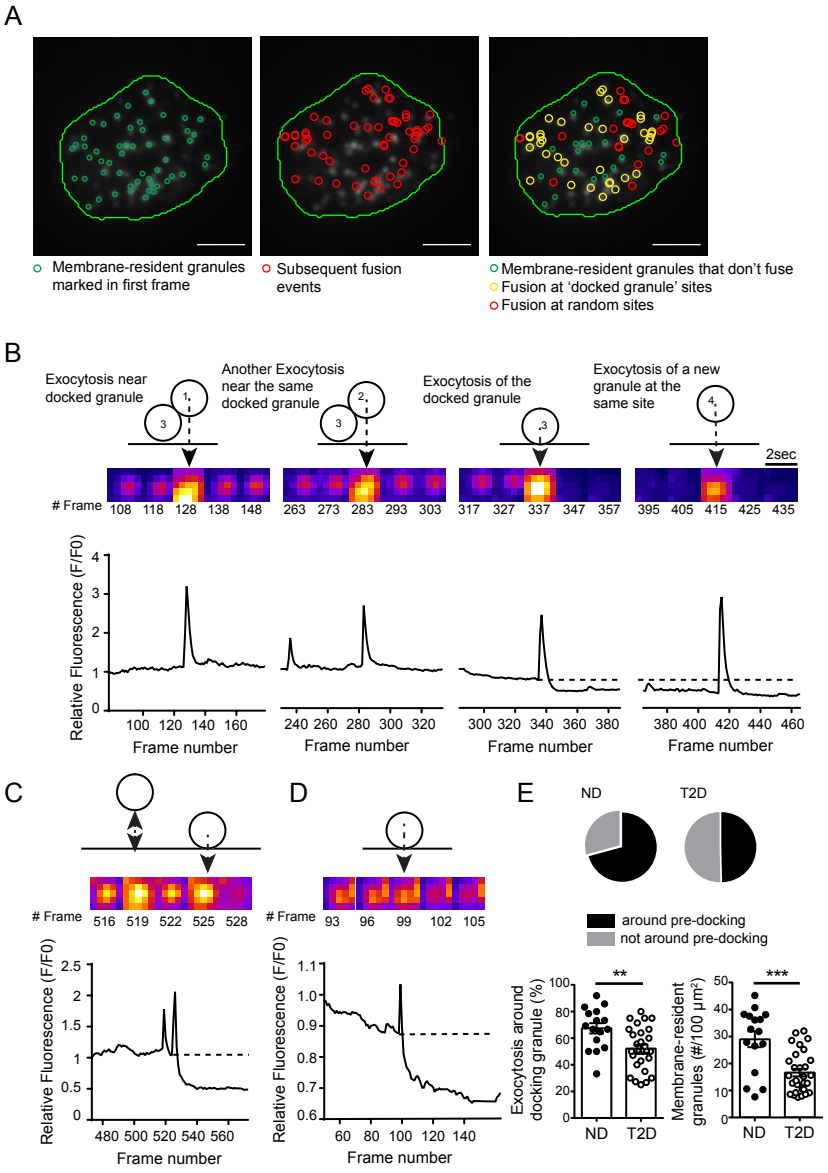

Figure. 4

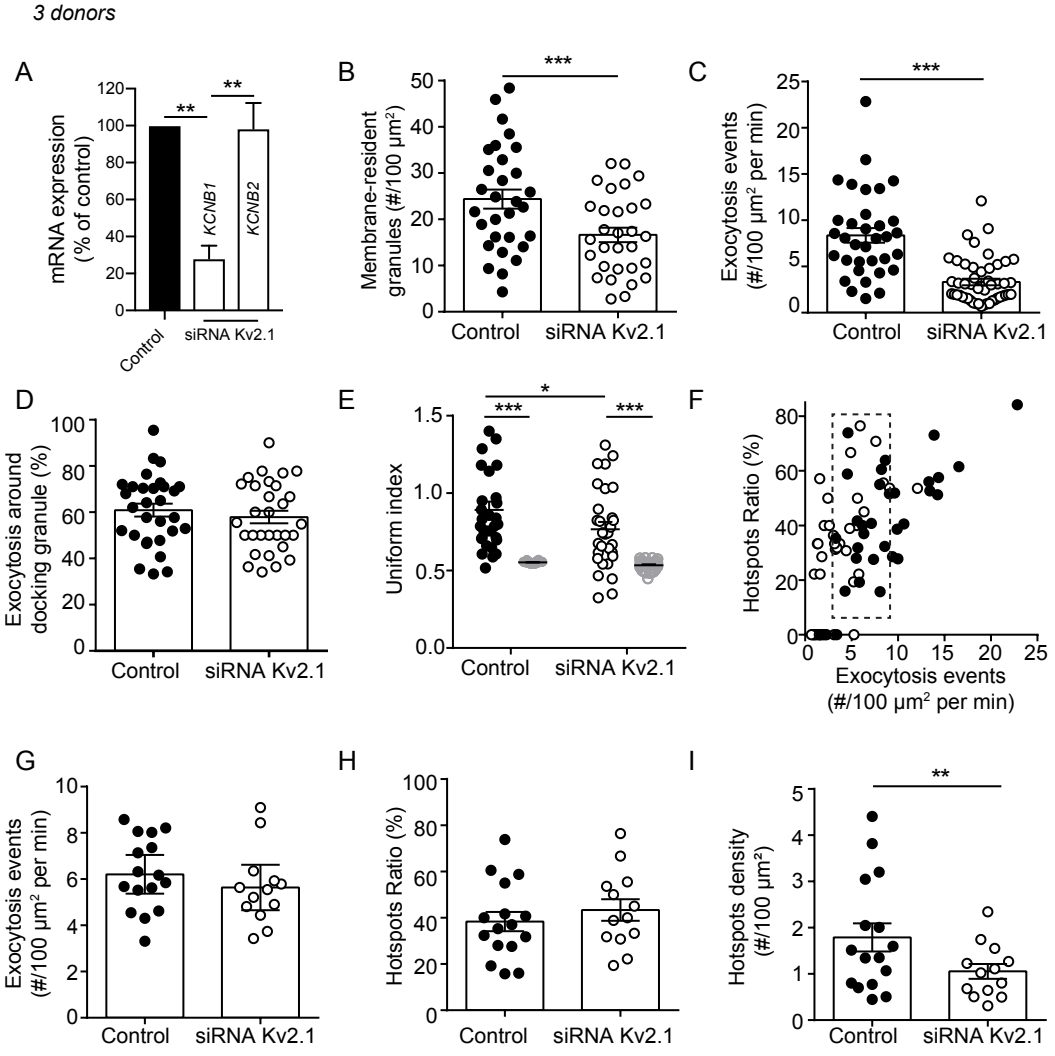

Figure. 5

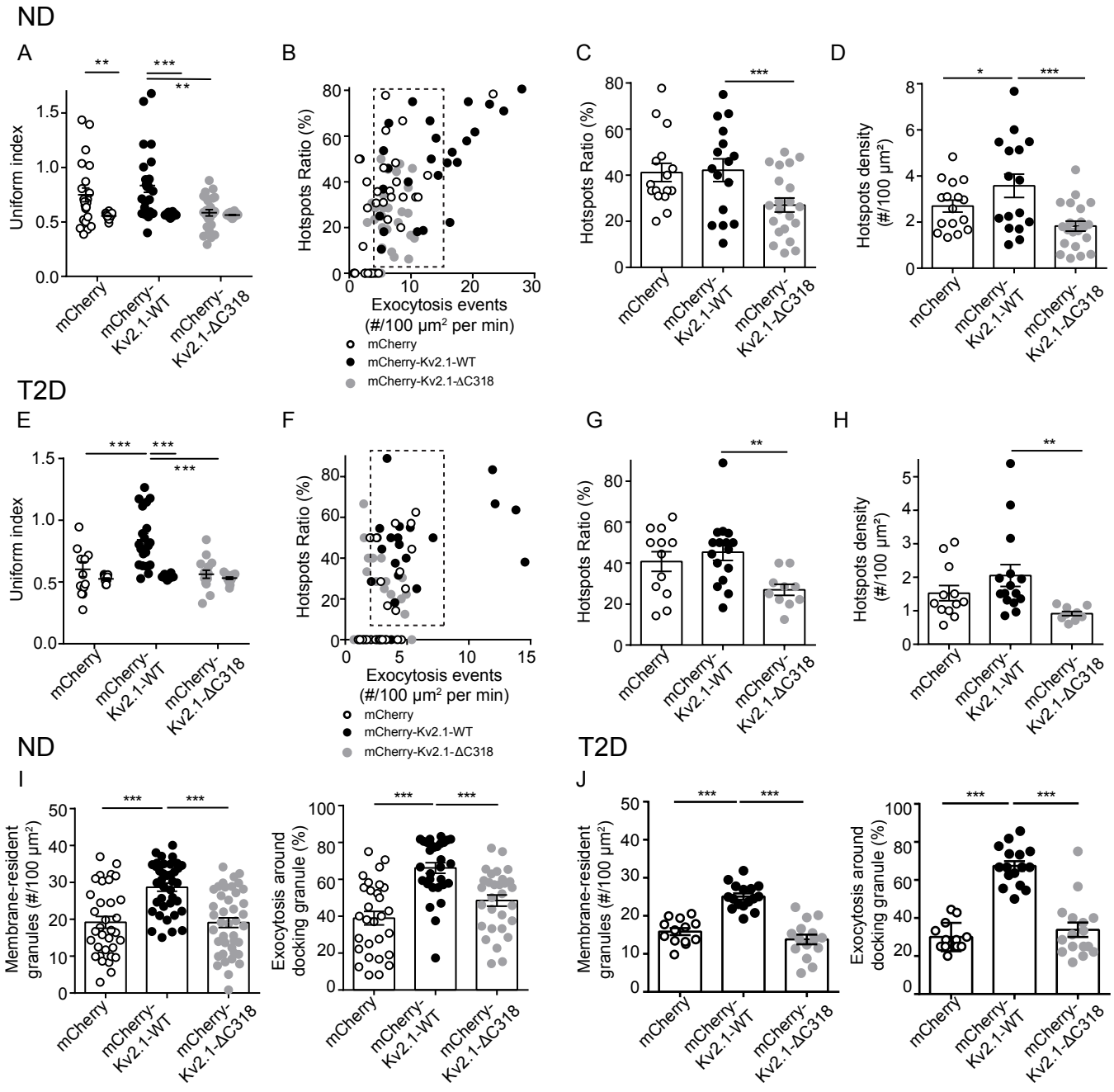

Figure. 6

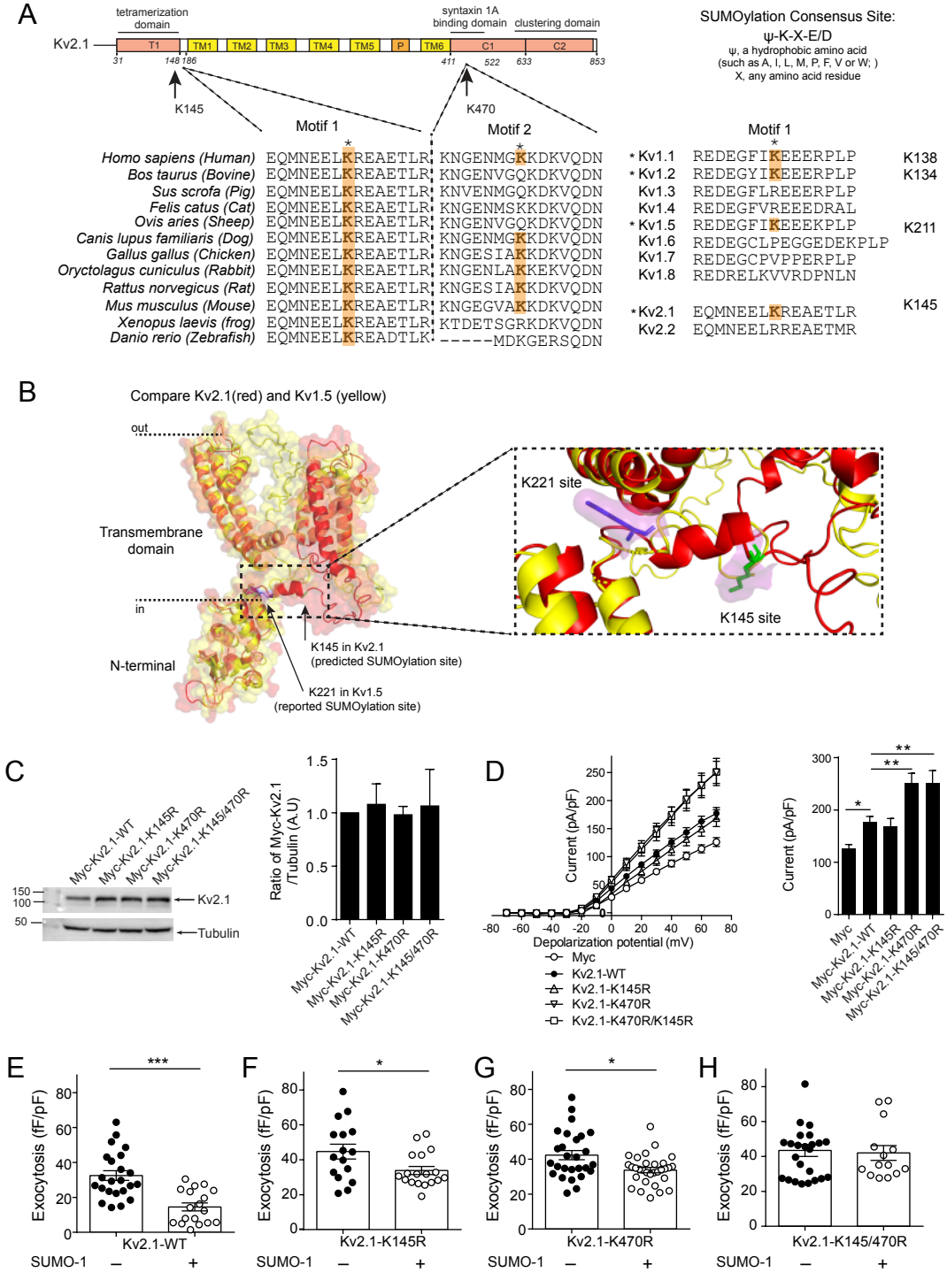

Figure. 7